

Spin-orbit driven phenomena in the isoelectronic $L1_0$ -Fe(Pd,Pt) alloys from first principles

J. Kudrnovský and V. Drchal

Institute of Physics, Academy of Sciences of the Czech Republic, Na Slovance 2, CZ-182 21 Praha 8, Czech Republic

I. Turek

Institute of Physics of Materials, Academy of Sciences of the Czech Republic, Žitkova 22, CZ-616 62 Brno, Czech Republic

(Received 7 November 2017; published 26 December 2017)

The anomalous Hall effect (AHE) and the Gilbert damping (GD) are studied theoretically for the partially ordered $L1_0$ -Fe(Pd,Pt) alloys. The varying alloy order and the spin-orbit coupling, which are due to the change in the Pd/Pt composition, allow for a chemical tuning of both phenomena which play an important role in the spintronic applications. The impact of the antisite disorder on the residual resistivity, AHE, and GD is studied from first principles using recently developed methods employing the Kubo-Bastin approach and the nonlocal torque operator method. The most interesting result is a different behavior of samples with low and high chemical orders. Good agreement between calculated and measured concentration trends is obtained for all quantities studied, while the absolute GD values are underestimated.

DOI: [10.1103/PhysRevB.96.214437](https://doi.org/10.1103/PhysRevB.96.214437)**I. INTRODUCTION**

The resistivity, anomalous Hall effect (AHE), and Gilbert damping (GD) are spin-orbit driven phenomena of great importance in future technological applications. The AHE [1] is closely related to the spin-transport phenomenon, and it is being intensively studied both experimentally and theoretically. In particular, a detailed understanding of the effect of disorder or the varying chemical composition is still a challenge for theory, in particular for its quantitative (first-principles) description in realistic materials. Experimentally, the measured AHE for disordered samples is often analyzed in terms of two contributions, one (skew-scattering term [2]) which depends strongly on the composition in the low-concentration limit and one which depends on concentrations very weakly. The latter contribution is, in some cases, decomposed into two parts, one obtained from the band structure calculations (intrinsic term [3]) and one named the side-jump term [4]. While such decomposition is attractive for interpretation, there is no simple and generally accepted way of how to realize it, in particular over the whole concentration range in alloys. This is also the case for the present $L1_0$ -Fe(Pd,Pt) alloy. Due to the sample preparation and annealing even the ideal $L1_0$ -FePd and $L1_0$ -FePt alloys contain some amount of disorder characterized by the long-range order (LRO) parameter S (see Ref. [5] for the general definition of the chemical order in the $L1_0$ alloys).

The ultrafast spin dynamics and related phenomena in ferromagnets can be well described by the phenomenological Landau-Lifshitz-Gilbert (LLG) equations. The LLG equations incorporate the GD term, which is an important phenomenological characteristic, although its reliable experimental determination is a difficult task, in particular the separation of the intrinsic and extrinsic parts. The theoretical estimate can thus be a useful tool as it can determine well-defined contributions, in particular the intrinsic ones. The intrinsic term in ideal metals arises from a combined effect of the spin-orbit coupling and temperature. The extrinsic term includes, e.g., the nonlocal relaxation processes which are relevant in thin films and multilayers, the effect of coverage layers and sample sizes, etc. On

the other hand, the GD is also strongly related to other physical parameters like the density of states at the Fermi energy and the electron relaxation time, which both vary strongly in the disordered alloys. The combination of the varying electron relaxation time and the spin-orbit coupling existing in the $L1_0$ -Fe(Pd,Pt) alloys offers a possibility for continuous tuning of the GD parameter. The role of temperature is, in such a case, of secondary importance; its effect is just superimposed on the effect of disorder and the spin-orbit coupling strength, and we will neglect it in this study for simplicity.

In the present study we wish to investigate, from first principles, the galvanomagnetic properties (the resistivity and the AHE) as well as the GD in the $L1_0$ -Fe(Pd,Pt) as a function of the chemical composition and varying order in the alloy as characterized by the LRO parameter S interpolating between the limits of a completely disordered system ($S = 0$) on one side and the highly ordered alloy (S close to 1) on the other side. The motivation comes from recent experiments with partially ordered $L1_0$ -Fe(Pd,Pt) alloys [6–8]. A gradual change in the Pd/Pt concentration also means varying influence of the spin-orbit strength in the alloy, which is a driving mechanism behind the AHE and GD phenomena. Finally, calculated and experimental results will be compared.

II. FORMALISM

The underlying electronic structure of the partially ordered $L1_0$ -Fe(Pd,Pt) alloy was studied using the Green's function formulation of the relativistic (Dirac) tight-binding linear muffin-tin orbital (TB-LMTO) method [9,10]. A possible effect of chemical disorder (varying alloy composition and different degrees of order on the $L1_0$ lattice) [5] was included in the framework of the coherent potential approximation (CPA) [9–11]. We employ the *spd* basis and Vosko-Wilk-Nusair exchange correlation potential [12], and we neglect changes of the lattice constant with the composition as well as possible small tetragonality of the lattice.

The transport properties are described by the conductivity tensor σ with components $\sigma_{\mu\nu}$ ($\mu, \nu = x, y, z$). They are cal-

culated in the framework of the Kubo-Bastin [13] formulation of the fully relativistic transport in disordered magnetic alloys, which includes both the Fermi-surface and Fermi-sea terms on equal footing. We refer the interested reader to our recent paper for details [14].

The diagonal components $\sigma_{\mu\mu}$ of the conductivity tensor determine the total conductivity σ_{tot} , while its off-diagonal component σ_{xy} is related to the anomalous Hall conductivity (AHC). A convention in which the magnetic moment points in the z direction (the direction of the fourfold rotation axis) is adopted. The total and anomalous Hall resistivities (AHR), ρ_{tot} and ρ_{xy} , respectively, are obtained by an inversion of the calculated conductivity tensor. The disorder-induced vertex corrections [15] are included. Their inclusion is simplified by the present formulation of the velocity as the intersite hopping [16], which leads to nonrandom velocity matrices. The disorder present in the system induces new contributions to the AHC, and their separation from the calculated total σ_{xy} is still a challenging problem. There have been attempts to separate out the skew-scattering and side-jump contributions [6,17,18] motivated by popular models [2,4] derived in the low-concentration limit, i.e., the case when the host system is a simple crystal without disorder. In the present case, on the contrary, we treat highly concentrated multisublattice alloys. We have suggested an alternative view [14] in which relevant contributions, namely, the coherent and vertex parts of the Fermi-surface and Fermi-sea terms, are collected into contributions invariant with respect to the choice of the TB-LMTO representation, which have a natural physical meaning [19]. In addition to the diagonal elements of the conductivity and the total σ_{xy} , we have (i) the vertex part of the Fermi-surface term of σ_{xy} and (ii) the sum of the coherent part of the Fermi-surface term and the total Fermi-sea contribution [14]. Thus, just the Fermi-sea term of σ_{xy} itself is not an invariant quantity. The vertex part of σ_{xy} is inversely proportional to the concentration in the low-concentration limit, and it is thus naturally related to the skew-scattering term and henceforth referred to as the extrinsic term. Numerous tests have shown a weak concentration dependence of term (ii), henceforth referred to as the intrinsic term. For the ideal crystal this term is equivalent to the AHC as obtained by the Berry-phase approach using conventional band structure methods. We will also neglect possible effects of the finite temperature on transport properties [20,21].

A recently developed nonlocal torque operator formulation of the GD is used to estimate the value of the dimensionless GD parameter α due to the alloy disorder. We refer to our recent paper for details [22]. The present approach leads to the non-site-diagonal and spin-independent effective spin-torque matrices, which simplifies evaluation of disorder-induced vertex corrections. It should be noted that vertex corrections play an essential role in the present formulation, and their neglect leads to quantitatively and physically incorrect results [22]. Our formulation gives results which compare well to other first-principles studies [23–25]. On the other hand, we again neglect temperature effects due to phonons and spin fluctuations [22,26] as their detailed inclusion is beyond the scope of the present study.

Experimentally, it is difficult to separate out the contribution due to the disorder from other contributions to the GD

(extrinsic terms). In real experiments there are a number of contributions not included in the present study, which concentrates on the damping due to disorder. In addition to already-mentioned temperature effect, we mention the thin-film geometry of the samples and its consequences, e.g., the radiative damping or the damping enhancement due to spin-pumping into the adjacent sample layer [27], the time-retardation process [28], the two-magnon scatterings, etc. On the other hand, knowledge of the intrinsic contribution due to the disorder may be useful in the atomistic simulations of the magnetization dynamics.

III. RESULTS AND DISCUSSION

A. Electronic structure

The relativistic TB-LMTO-CPA approach provides necessary inputs for the transport and GD calculations based thus on a unified model. The distribution of Fe/Pd/Pt atoms on the native Fe and Pd/Pt sublattices which form the $L1_0$ lattice is influenced by sample preparation and annealing and can be characterized by the LRO parameters S and Pt concentration. The LRO parameter S is defined as $S = 1 - 2x_{\text{as}}$, where x_{as} is the concentration of the antisite atoms, i.e., Fe atoms on the native Pd/Pt sublattice and Pd/Pt atoms on the native Fe sublattice. The values of S range from $S = 0$ for a completely disordered fcc $\text{Fe}_{0.5}(\text{Pd}_{1-x}, \text{Pt}_x)_{0.5}$ alloy to $S = 1$ for well-ordered $L1_0$ -Fe(Pd,Pt) alloys which include the ideal $L1_0$ -FePd and $L1_0$ -FePt alloys as a special limit. An unknown parameter is the ratio of the antisite Pd and Pt atoms on the native Fe lattice for a given S and Pt concentration. We have chosen the simplest model, namely, that Pd/Pt atoms occupy the Fe sublattice in the ratio of their concentrations x_{Pt} and $y_{\text{Pd}} = 1 - x_{\text{Pt}}$. In other words, we have not considered a preferential occupation of Pd or Pt atoms on the Fe sublattice. In principle, one cannot exclude such preferential occupation. However, its quantitative study is a difficult thermodynamic and kinetic problem depending on the sample preparation conditions and the temperature. Such a problem, although an interesting one, is beyond the scope of the present paper.

Alloys are ferromagnetic with dominating Fe moments and small induced moments on the Pd and Pt atoms. The Fe moments weakly depend on the order and alloy composition and are around $3.25\mu_B$ to $3.35\mu_B$. Induced moments on Pd/Pt atoms are an order of magnitude smaller ($0.3\mu_B$ to $0.4\mu_B$) and similar for both atoms.

B. Residual resistivity

The total resistivities for $L1_0$ -Fe(Pd $_{1-x}$,Pt $_x$) alloys over the whole concentration range of Pt atoms ranging from disordered samples ($S = 0$ and 0.5) to well-ordered ones ($S = 0.8, 0.85, 0.9$, and 0.975) were calculated. Specifically, the $L1_0$ -FePd/ $L1_0$ -FePt ordered alloys were simulated by Pt concentrations of 0.01 and 0.99, respectively, and the high $S = 0.975$.

Calculated residual resistivities are shown in Fig. 1. There is a natural increase of resistivities with decreasing order (decreasing values of S) that reaches its maximum for a completely disordered case ($S = 0$) corresponding to fcc $\text{Fe}_{0.5}(\text{Pd}_{1-x}, \text{Pt}_x)_{0.5}$. We have verified that a monotonic

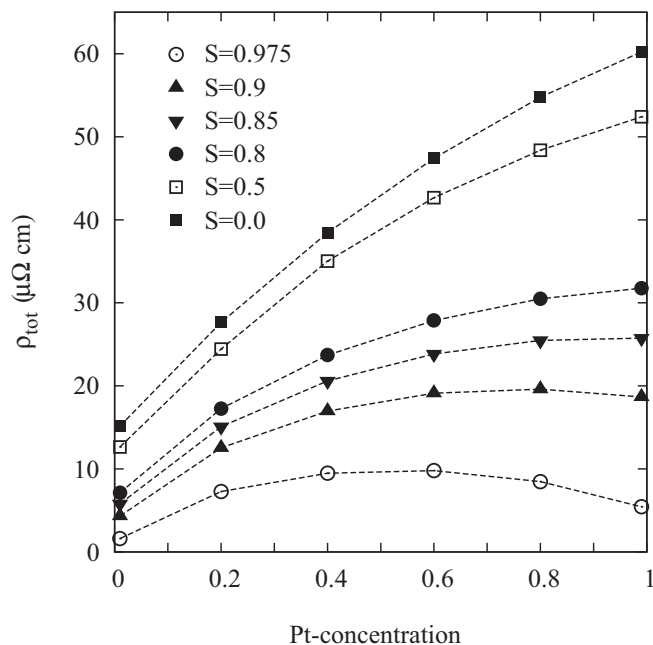


FIG. 1. Total resistivities ρ_{tot} of $L1_0\text{-Fe}(\text{Pd}_{1-x},\text{Pt}_x)$ alloys as functions of the Pt concentration x for various chemical orders characterized by the LRO parameter S . Note that the $x = 0.01$ and $x = 0.99$ cases describe the limits of the ideal $L1_0\text{-FePd}$ and $L1_0\text{-FePt}$ alloys, respectively.

increase of ρ_{tot} with increasing Pt content for the disordered limit ($S = 0$) was also obtained in the scalar-relativistic case, although the absolute values of ρ_{tot} are larger in the relativistic case due to the mixing of both spin channels by spin-orbit coupling. For example, ρ_{tot} for scalar-relativistic fcc ($\text{Fe}_{0.5},\text{Pd}_{0.5}$) and fcc ($\text{Fe}_{0.5},\text{Pt}_{0.5}$) alloys are about 10 and 49 $\mu\Omega$ cm, which has to be compared to about 15 and 60 $\mu\Omega$ cm for the relativistic case (see Fig. 1) [29]. On the other hand, for an almost perfect case ($S = 0.975$) the effect of disorder is concentrated mostly on the (Pd,Pt) sublattice, while the Fe sublattice is almost perfect. This resembles a conventional binary alloy and results in the parabolic Nordheim-like concentration behavior (characteristic for a weak disorder) with the maximum roughly in the middle of the concentration range. Remaining cases of S interpolate between the above two limits.

One can distinguish two regions, one for S roughly up to 0.8, in which ρ_{tot} increases monotonically with the Pt concentration, and the other with a nonmonotonic behavior with resistivity maxima for x between 0.6 and 0.8 ($S > 0.8$). Calculated ρ_{tot} as a function of x for $S = 0$ interpolates between the disordered fcc ($\text{Fe}_{0.5},\text{Pd}_{0.5}$) and the disordered fcc ($\text{Fe}_{0.5},\text{Pt}_{0.5}$). The experiment at zero temperature [6] shows the ρ_{tot} maximum around 25–30 $\mu\Omega$ cm at $x = 0.65$. Calculated ρ_{tot} (around 20–25 $\mu\Omega$ cm) for $S = 0.9\text{--}0.85$ are in good agreement with the experiment, while the maxima are shifted to higher S (the experimental estimate of S is about $S = 0.8 \pm 0.1$ for annealed samples). Resistivities ρ_{tot} for the Pd-rich region are smaller than the Pt-rich one, again in agreement with the experiment. We can conclude that the experiment can be understood as a combination of two effects,

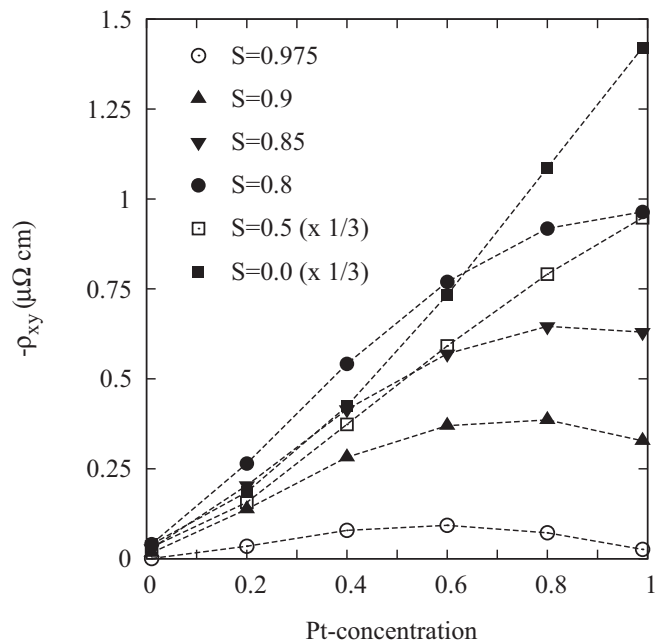


FIG. 2. Anomalous Hall resistivities ρ_{xy} of $L1_0\text{-Fe}(\text{Pd}_{1-x},\text{Pt}_x)$ alloys are shown as functions of the Pt concentration x for various chemical orders as characterized by the LRO parameter S . Note that the $x = 0.01$ and $x = 0.99$ cases describe the limits of the ideal $L1_0\text{-FePd}$ and $L1_0\text{-FePt}$ alloys, respectively.

namely, the effective spin-orbit coupling (increasing with x) and the chemical disorder modified by the LRO effects.

The experiment [6] also shows a parabolic-like increase of resistivities with temperature up to the room temperature. Although we have not calculated the dependence of ρ_{tot} on the temperature explicitly, one can speculate about a dominating effect of spin fluctuations compared to the effect of phonons as the latter will lead to a linear increase of ρ_{tot} with the temperature [20,21].

C. Anomalous Hall effect

As a first step we compare the AHC values σ_{xy} for $L1_0\text{-FePd}$ and $L1_0\text{-FePt}$ samples measured in the experiment [30] and compare them with calculated ones. The experimental values are 806 ± 18 and 1267 ± 101 S/cm, respectively. These values compare very well with the calculated values for $S = 0.8$ and 0.85 , namely, 805 and 856 S/cm for $L1_0\text{-FePd}$ and 1158 and 1181 S/cm for $L1_0\text{-FePt}$. We note that the present result for $x = 0.99$ agrees, as expected, with results obtained in our previous study of the ideal $L1_0\text{-FePt}$ alloy [31].

The calculated AHR ρ_{xy} for $L1_0\text{-Fe}(\text{Pd}_{1-x},\text{Pt}_x)$ alloys as a function of x and S is shown in Fig. 2. The concentration trend is similar to that for ρ_{tot} , and its origins are the same: an interplay of chemical disorder and varying effective spin-orbit coupling. This is formally seen from the relation $\rho_{xy} \approx \sigma_{xy}/(\sigma_{\text{tot}})^2$ with changes induced by quadratic dependence on the resistivity (conductivity). One thus again distinguishes regions of low ordering ($S = 0$ and 0.5) with a monotonic increase of the AHR (note a factor of 1/3 in Fig. 2) which is contrasted with a nonmonotonic behavior with local maxima

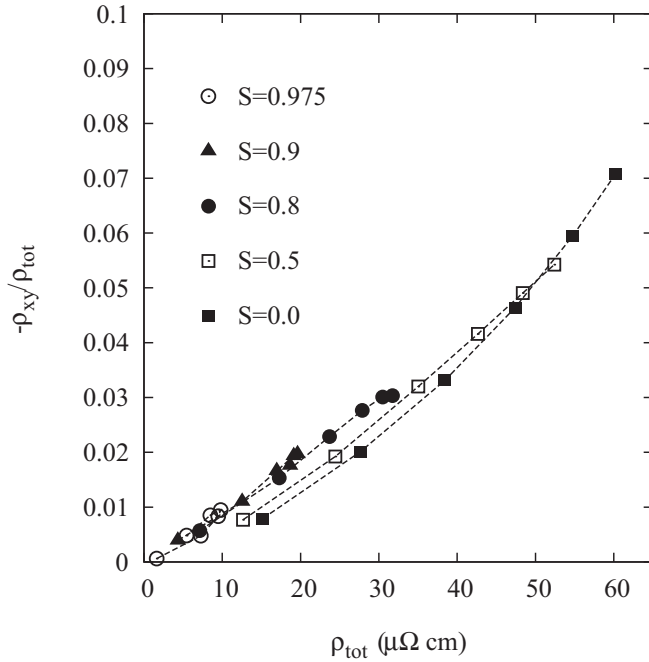


FIG. 3. The quantity ρ_{xy}/ρ_{tot} is plotted as a function of ρ_{tot} for a set of $L1_0\text{-Fe}(\text{Pd}_{1-x},\text{Pt}_x)$ alloys corresponding to various values of the chemical order characterized by the LRO parameter S . The linear dependence characterizes a dominating intrinsic character of the scattering mechanism in a given alloy.

for well-ordered samples ($S > 0.8$). The experiment ($S = 0.8 \pm 0.1$) shows a maximum at x around 0.65. The calculated AHR value around $0.65 \mu\Omega \text{ cm}$ (for $S = 0.85$) is in good agreement with the experiment, although again the maximum is shifted to a higher x .

The experimental values of ρ_{xy} are often decomposed into an extrinsic (skew-scattering) term (proportional to ρ_{tot} or ρ_{xx}) and an intrinsic term (including the side-jump contribution) proportional to $(\rho_{tot})^2$, i.e., $\rho_{xy} = A\rho_{tot} + B(\rho_{tot})^2$, where A and B are fitted constants (see, e.g., Ref. [31]). To this end we plot in Fig. 3 the dependence ρ_{xy}/ρ_{tot} as a function of ρ_{tot} for the present alloy. Disordered samples ($S = 0$ and partly also $S = 0.5$) clearly show a deviation from the ideal intrinsic behavior (a linear dependence), while the intrinsic behavior dominates for well-ordered alloys. The above linear dependence was also found experimentally for $L1_0\text{-FePd/FePt}$ alloys with $S = 0.8 \pm 0.1$ [30].

The authors of Ref. [30] have also suggested the decomposition of such dependence into intrinsic, skew-scattering, and side-jump contributions. Instead of that we present in Fig. 4 the concentration dependence of the extrinsic part σ_{xy}^{ext} of AHC (the vertex part of the Fermi-surface contribution to the σ_{xy}). The values of σ_{xy} are quite large, being between 800 and 1200 S/cm. Most of the values of the extrinsic part σ_{xy}^{ext} shown in Fig. 4 are around 100 S/cm and thus quite small, indicating the prevailing intrinsic character of σ_{xy} . The noticeable exception is the highly ordered case ($S = 0.975$), in particular for very low defect concentrations ($x = 0.01$ and 0.99) for which the extrinsic contribution is non-negligible. This can be considered an almost textbook example of a strong skew-scattering contribution. A similar result was obtained

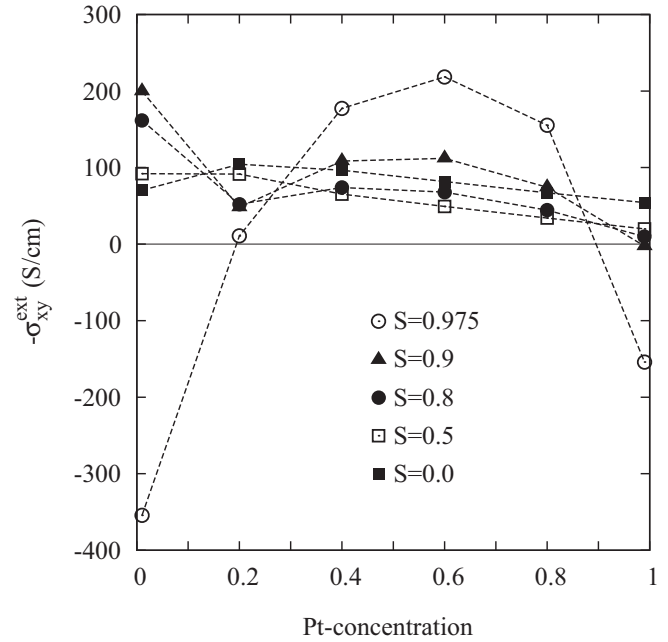


FIG. 4. The extrinsic part σ_{xy}^{ext} of σ_{xy} for $L1_0\text{-Fe}(\text{Pd}_{1-x},\text{Pt}_x)$ alloys, i.e., the incoherent part of the Fermi-surface term, is plotted as a function of the Pt concentration x for various chemical orders characterized by the LRO parameter S . Note that the $x = 0.01$ and $x = 0.99$ cases describe the limits of the ideal $L1_0\text{-FePd}$ and $L1_0\text{-FePt}$ alloys, respectively. For a comparison, the values of the total σ_{xy} range from about 800 to 1200 S/cm for the ideal $L1_0\text{-FePd}$ and $L1_0\text{-FePt}$ alloys, respectively.

also in Ref. [31] for a highly ordered $L1_0\text{-FePt}$ with a small antisite disorder.

D. Gilbert damping

Measurement of the GD constants is a delicate experiment in which different methods, e.g., the ferromagnetic resonance [32] and the time-resolved magneto-optical Kerr effect [33], are employed. The experimental samples depend on the preparation, e.g., on the amount of disorder due to the annealing temperature, the sample shape (bulk or thin layer), the temperature of measurement, and other factors, and as mentioned in the Introduction they are the reason for often very small values of the calculated GD parameter α . In the present study we concentrate on the intrinsic effect of the disorder as the studied partly ordered $L1_0\text{-Fe}(\text{Pd,Pt})$ alloy contains various amounts of disorder due to sample preparations. The studied system even contains the disorder intentionally as the increasing Pt content increases the effective spin-orbit coupling in the sample, which is the driving mechanism behind the GD phenomena.

Specific cases of the fully ordered $L1_0\text{-FePd}$ and $L1_0\text{-FePt}$ alloys are shown in Fig. 5. They, in fact, correspond to $x = 0.01$ and $x = 0.99$, respectively, to avoid the perfectly ordered alloys with theoretically infinite GD parameters α at zero temperature assumed in the present study. The $L1_0\text{-FePd}$ alloy shows almost the same GD values between $S = 0$ and $S = 0.5$ and their weak decrease with increasing order, as seen in Fig. 5. This trend agrees with both the experiment and

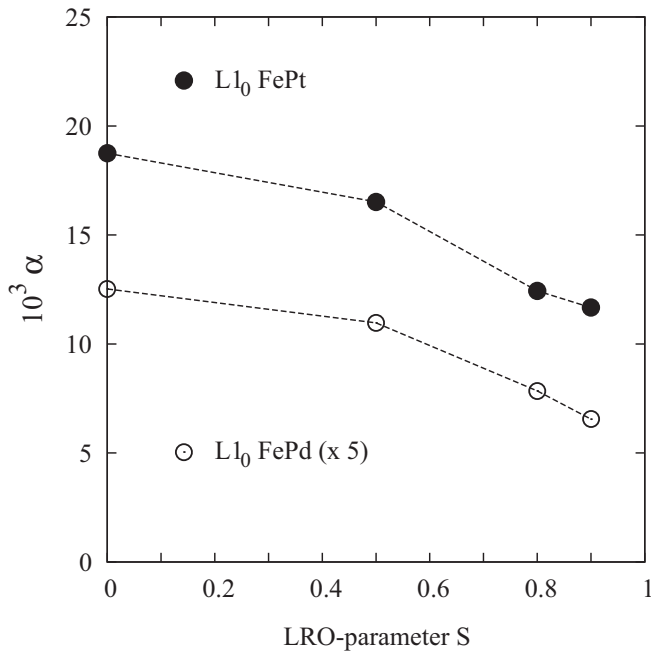


FIG. 5. Calculated dimensionless GD parameters α as functions of the LRO parameter S for the ordered $L1_0$ -FePd and $L1_0$ -FePt alloys described as $L1_0$ -Fe(Pd_{1-x},Pt_x) alloys with the Pt concentrations $x = 0.01$ and $x = 0.99$, respectively. The GD parameter α of the $L1_0$ -FePd is multiplied by a factor of 5.

related theoretical calculations [34]. The theoretical values of α , ranging from 0.001 to 0.0025, are, however, smaller than those of the experiment (0.002 to 0.007).

The effect of atomic order on the GD damping of the $L1_0$ -FePt alloy was studied earlier by Sakuma [24] and by the present authors [22]. The impact of the LRO (antisite disorder) was also recently studied experimentally [35]. A roughly linear increase in the GD parameter α with the disorder or, alternatively, with the decreasing LRO parameter S (from $S = 0.94$ to $S = 0.68$) was obtained. The overall trend is thus the same as for the $L1_0$ -FePd alloy and in agreement with the experiment, but calculated GD values are much larger than the values obtained for the $L1_0$ -FePd alloy due to a stronger spin-orbit coupling in $L1_0$ -FePt (note a scaling factor of 5 for the $L1_0$ -FePd alloy in Fig. 5). The calculated GD values are, however, much smaller than the experimental ones (0.01 to 0.08). Similar values of the GD parameter α (0.04 to 0.1) were reported by other groups [36,37]. As discussed in the Introduction, the present theory captures just the intrinsic part of the GD due to the alloy disorder.

A linear concentration trend of GD parameters α in disordered fcc Fe_{0.5}(Pd_{1-x},Pt_x)_{0.5} alloys was observed experimentally [8], although the authors do not specify the amount of disorder (a value of the LRO parameter S). Most likely, such a result is valid not strictly for $S = 0$ but also for a small order (say, $S < 0.5$ or so). Such behavior is in full agreement with the present calculations ($S = 0$) shown in Fig. 6. A monotonic linear increase in the GD parameters α with x is simply a consequence of the increase in the effective spin-orbit strength due to Pt atoms. Calculated values of the GD parameter α

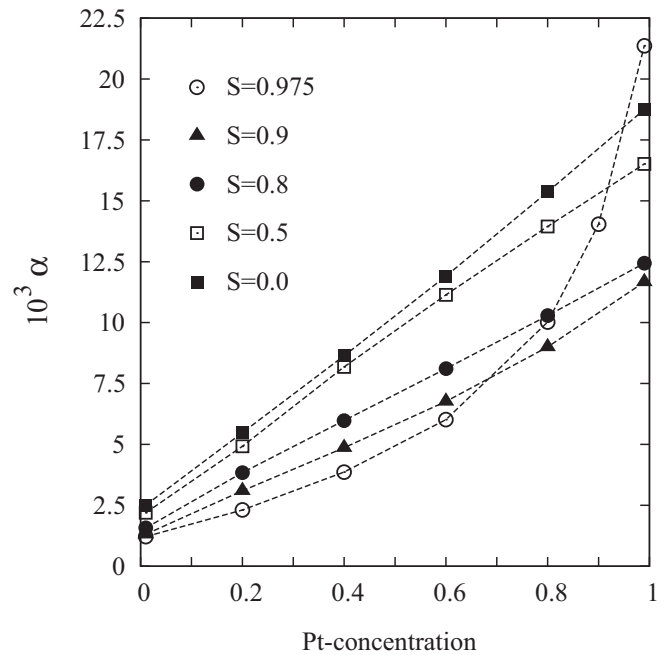


FIG. 6. Calculated dimensionless GD parameters α of $L1_0$ -Fe(Pd_{1-x},Pt_x) alloys as functions of the Pt concentration x for various chemical orders characterized by the LRO parameter S . Note that the $x = 0.01$ and $x = 0.99$ cases describe the limits of the ideal $L1_0$ -FePd and $L1_0$ -FePt alloys, respectively.

ranging from 0.002 to 0.018 are smaller than experimental ones (ranging from less than 0.01 up to 0.04).

On the contrary, for a higher ordering, namely, $S = 0.9$ and $S = 0.975$ in particular, we observe a nonlinear, parabolic-like increase of GD parameters α . It should be ascribed to a relatively large GD of the ideal $L1_0$ -FePt alloy (see also Fig. 5) when approaching large Pt concentrations. Clearly, alloying of elements with different spin-orbit couplings allows one to manipulate the GD parameters in a relatively large window of their values. In Ref. [7] a well-ordered $L1_0$ -Fe(Pd,Pt) alloy was studied experimentally; the authors estimated the LRO parameter S to be about 0.8, although its exact determination is a delicate task, so this value should not be taken too literally. The experiment shows, in contrast to the disordered counterpart [8], the nonlinear weakly parabolic dependence of the GD parameter α on increasing Pt content. Such behavior is in agreement with the concentration trend obtained with the present calculations for well-ordered samples (one could estimate an optimal value for S as being slightly larger than $S = 0.9$). Considering experimental uncertainty with regard to the exact experimental value of S , it is an acceptable agreement. On the other hand, calculated values, in particular for a large Pt content, are too small, as already discussed above for the $L1_0$ -FePt alloy: The experimental GD parameter α increases up to 0.1.

We note that a similar concentration trend was also reproduced theoretically in Ref. [7]. The authors even obtained quantitative agreement of the calculated GD parameters α , but using a phenomenological relaxation time simulating both the amount of order and Pt concentration

in the framework of the breathing Fermi-surface model of Kamberský and Gilmore [38].

IV. CONCLUSIONS

We have presented results of a first-principles study of the galvanomagnetic properties and Gilbert damping parameters of the $L1_0$ -Fe(Pd $_{1-x}$,Pt $_x$) alloys. To this end we used a recently developed Kubo-Bastin transport theory and the nonlocal torque operator approach for the Gilbert damping formulated in the framework of the TB-LMTO method. The variable Pd/Pt content allowed us to study the combined effect of disorder and spin-orbit coupling strength on the above spin-driven phenomena. In addition, as an external parameter, we varied the partial long-range order in samples originating in their annealing. While the real experimental samples discussed in this study have a relatively large order characterized by the long-range order parameter $S = 0.8 \pm 0.1$, we present results for samples ranging from a completely disordered alloy ($S = 0$) up to well-ordered ones with $S = 0.975$. The main conclusions are as follows: (i) The total (longitudinal) and anomalous Hall resistivities exhibit different behavior as functions of the Pt content, namely, the monotonic increase for samples with low order ($S = 0$ and 0.5) and nonmonotonic one with local maxima for large Pt content for $S > 0.8$. Calculated

trends and values agree well with the experiment, although the local maxima are shifted to slightly larger Pt concentrations. (ii) Well-ordered samples ($S \geq 0.8$) exhibit a dominating intrinsic character for the AHC, while disordered samples show some deviations. Such different behavior is clearly seen when plotting the extrinsic contribution to the AHC (the vertex part of the Fermi-surface term) over the whole range of parameters. The largest extrinsic contributions correspond to $x = 0.01$ and 0.99 for a highly ordered sample ($S = 0.975$). (iii) Finally, the GD parameter also exhibits different concentration trends, namely, a linear dependence on x for disordered samples and a nonlinear, parabolic-like behavior for well-ordered samples. Such trends are in agreement with experiments for disordered and well-ordered samples. On the other hand, the calculated values of the GD parameters, in particular at the Pt-rich end, are too small compared to the experiment because of the neglect of extrinsic contributions, including the effect of temperature.

ACKNOWLEDGMENTS

The authors acknowledge the financial support from the Czech Science Foundation (Grant No. 15-13436S) and the National Grid Infrastructure MetaCentrum (Project No. LM2015042) for access to computation facilities.

-
- [1] N. Nagaosa, J. Sinova, S. Onoda, A. H. MacDonald, and N. P. Ong, *Rev. Mod. Phys.* **82**, 1539 (2010).
- [2] J. Smit, *Physica* **24**, 39 (1958).
- [3] R. Karplus and J. M. Luttinger, *Phys. Rev.* **95**, 1154 (1954).
- [4] L. Berger, *Physica* **30**, 1141 (1964).
- [5] J. Banhart and G. Czycholl, *Europhys. Lett.* **58**, 264 (2002).
- [6] P. He, L. Ma, Z. Shi, G. Y. Guo, J.-G. Zheng, Y. Xin, and S. M. Zhou, *Phys. Rev. Lett.* **109**, 066402 (2012).
- [7] P. He, X. Ma, J. W. Zhang, H. B. Zhao, G. Lüpke, Z. Shi, and S. M. Zhou, *Phys. Rev. Lett.* **110**, 077203 (2013).
- [8] L. Ma, S. F. Li, P. He, W. J. Fan, X. G. Xu, Y. Jiang, T. S. Lai, F. L. Chen, and S. M. Zhou, *J. Appl. Phys.* **116**, 113908 (2014).
- [9] I. Turek, V. Drchal, J. Kudrnovský, M. Šob, and P. Weinberger, *Electronic Structure of Disordered Alloys, Surfaces and Interfaces* (Kluwer, Boston, 1997).
- [10] A. B. Shick, V. Drchal, J. Kudrnovský, and P. Weinberger, *Phys. Rev. B* **54**, 1610 (1996).
- [11] I. Turek, J. Kudrnovský, and K. Carva, *Phys. Rev. B* **86**, 174430 (2012).
- [12] S. H. Vosko, L. Wilk, and M. Nusair, *Can. J. Phys.* **58**, 1200 (1980).
- [13] A. Bastin, C. Lewiner, O. Betbeder-Matibet, and P. Nozieres, *J. Phys. Chem. Solids* **32**, 1811 (1971).
- [14] I. Turek, J. Kudrnovský, and V. Drchal, *Phys. Rev. B* **89**, 064405 (2014).
- [15] K. Carva, I. Turek, J. Kudrnovský, and O. Bengone, *Phys. Rev. B* **73**, 144421 (2006).
- [16] I. Turek, J. Kudrnovský, V. Drchal, L. Szunyogh, and P. Weinberger, *Phys. Rev. B* **65**, 125101 (2002).
- [17] B. Zimmermann, K. Chadova, D. Ködderitzsch, S. Blügel, H. Ebert, D. V. Fedorov, N. H. Long, P. Mavropoulos, I. Mertig, Yu. Mokrousov, and M. Gradhand, *Phys. Rev. B* **90**, 220403(R) (2014).
- [18] K. Hyodo, A. Sakuma, and Y. Kota, *Phys. Rev. B* **94**, 104404 (2016).
- [19] The Kubo-Greenwood conductivity is naturally separated into parts describing uncorrelated (coherent) and correlated (vertex) two-particle quantities with respect to the configurational averaging. The vertex part corresponds to the back-scattering part of the conventional Boltzmann equation. The physically relevant parts of the conductivity tensor are those which are invariant with respect to different LMTO transformations, as shown in detail in Ref. [14].
- [20] D. Ködderitzsch, K. Chadova, J. Minar, and H. Ebert, *New J. Phys.* **15**, 053009 (2013).
- [21] D. Wagenknecht, K. Carva, and I. Turek, *IEEE Trans. Magn.* **53**, 1700205 (2017).
- [22] I. Turek, J. Kudrnovský, and V. Drchal, *Phys. Rev. B* **92**, 214407 (2015).
- [23] A. A. Starikov, P. J. Kelly, A. Brataas, Y. Tserkovnyak, and G. E. W. Bauer, *Phys. Rev. Lett.* **105**, 236601 (2010).
- [24] A. Sakuma, *J. Phys. Soc. Jpn.* **81**, 084701 (2012).
- [25] S. Mankovsky, D. Ködderitzsch, G. Woltersdorf, and H. Ebert, *Phys. Rev. B* **87**, 014430 (2013).
- [26] H. Ebert, S. Mankovsky, K. Chadova, S. Polesya, J. Minár, and D. Ködderitzsch, *Phys. Rev. B* **91**, 165132 (2015).
- [27] M. A. W. Schoen, J. Lucassen, H. T. Nembach, B. Koopmans, T. J. Silva, C. H. Back, and J. M. Shaw, *Phys. Rev. B* **95**, 134411 (2017).
- [28] D. Thonig, J. Henk, and O. Eriksson, *Phys. Rev. B* **92**, 104403 (2015).

- [29] One would expect similar resistivities of FePd and FePt for $S = 0$ because Pd and Pt are isoelectronic elements. It follows from calculated scalar-relativistic densities of states that the Fermi energy lies in the sp band for FePd but partly in the d band for FePt. This is a consequence of a broader d band in the FePt alloy. The larger majority conductivity of FePd compared to FePt reflects weaker scattering and larger electron velocity in the sp band compared to the d band. This, together with similar minority resistivities, explains a larger resistivity in FePt which is not qualitatively changed by the spin-orbit coupling.
- [30] K. M. Seemann, Y. Mokrousov, A. Aziz, J. Miguel, F. Kronast, W. Kuch, M. G. Blamire, A. T. Hindmarch, B. J. Hickey, I. Souza, and C. H. Marrows, *Phys. Rev. Lett.* **104**, 076402 (2010).
- [31] J. Kudrnovský, V. Drchal, and I. Turek, *Phys. Rev. B* **89**, 224422 (2014).
- [32] B. Heinrich, in *Ultrathin Magnetic Structures II*, edited by B. Heinrich and J. A. C. Bland (Springer, Berlin, 1994), p. 195.
- [33] S. Iihama, S. Mizukami, H. Naganuma, M. Oogane, Y. Ando, and T. Miyazaki, *Phys. Rev. B* **89**, 174416 (2014).
- [34] S. Iihama, A. Sakuma, H. Naganuma, M. Oogane, S. Mizukami, and Y. Ando, *Phys. Rev. B* **94**, 174425 (2016).
- [35] X. Ma, L. Ma, P. He, H. B. Zhao, S. M. Zhou, and G. Lüpke, *Phys. Rev. B* **91**, 014438 (2015).
- [36] S. Mizukami, S. Iihama, N. Inami, T. Hiratsuka, G. Kim, H. Naganuma, M. Oogane, and Y. Ando, *Appl. Phys. Lett.* **98**, 052501 (2011).
- [37] Z. Chen, M. Yi, M. Chen, S. Li, S. Zhou, and T. La, *Appl. Phys. Lett.* **101**, 222402 (2012).
- [38] K. Gilmore, Y. U. Idzerda, and M. D. Stiles, *J. Appl. Phys.* **103**, 07D303 (2008).